Chemical Science

Accepted Manuscript

Volume 9
Number 1
7 January 2018
Pages 1-268

Chemical Science

rsc.li/chemical-science

ISSN 2041-6539

EDGE ARTICLE
Xinjing Tang et al.
Caged circular siRNAs for photomodulation of gene
expression in cells and mice

ROYAL SOCIETY
OF CHEMISTRY

This is an Accepted Manuscript, which has been through the Royal Society of Chemistry peer review process and has been accepted for publication.

Accepted Manuscripts are published online shortly after acceptance, before technical editing, formatting and proof reading. Using this free service, authors can make their results available to the community, in citable form, before we publish the edited article. We will replace this Accepted Manuscript with the edited and formatted Advance Article as soon as it is available.

You can find more information about Accepted Manuscripts in the Information for Authors.

Please note that technical editing may introduce minor changes to the text and/or graphics, which may alter content. The journal's standard Terms & Conditions and the Ethical guidelines still apply. In no event shall the Royal Society of Chemistry be held responsible for any errors or omissions in this Accepted Manuscript or any consequences arising from the use of any information it contains.

ROYAL SOCIETY
OF CHEMISTRY

rsc.li/chemical-science

Efficient Trinuclear Ru(II)-Re(I) Supramolecular Photocatalysts for CO$_2$ Reduction Based on a New Tris-chelating Bridging Ligand Build Around a Central Aromatic Ring

Ambra M. Cancelliere,[a] Fausto Puntoriero,[a] Scolastica Serroni,[a] Sebastiano Campagna,,[a] Yusuke Tamaki,[b] Daiki Saito[b] and Osamu Ishitani*,[b]*

(a) Dipartimento di Scienze Chimiche, Biologiche, Farmaceutiche ed Ambientali, Università di Messina and Centro di Ricerca Interuniversitario per la conversione chimica dell'energia solare (SOLAR-CHEM, sezione di Messina), Viale Ferdinando Stagno d'Alcontres, 31 – 98166, Messina, Italy.

(b) Department of Chemistry, School of Science, Tokyo Institute of Technology, 2-12-1-NE-1, O-okayama, Meguro-ku, Tokyo, 152-8550, Japan.

Abstract

We have designed and synthesized a new tris-chelating polypyridine ligand (**bpy₃Ph**) suitable to be used as bridging ligand (BL) for constructing various supramolecular photocatalysts. This BL is a phenylene ring with three ethylene chains in 1, 3, and 5 positions, of which the other terminals are connected to 2,2'-bipyridine moieties. The ligand **bpy₃Ph** has been used to prepare, according to a multi-step synthetic protocol, trinuclear supramolecular photocatalysts containing different metal subunits. In particular, the compounds **Ru2Re** and **RuRe2** have been prepared, containing different ratios of components based on $Ru(dmb)_3^{2+}$-type and $Re(dmb)(CO)_3Cl$-type units (dmb = 4,4'-dimethyl-2,2'-bipyridine), which can play the roles of photosensitizers and catalysts units for photocatalytic CO_2 reduction, respectively. The trinuclear model **Ru3** and the mononuclear and dinuclear **Ru** and **Ru2** precursor metal complexes, containing free chelating sites, have also been synthesized using the same bridging ligand. The absorption spectra, redox behaviour and photophysical properties of the new species indicates that there is no strong electronic interaction among the Ru and Re units. The trinuclear complexes **Ru2Re** and **RuRe2** could photocatalyze CO_2 reduction to CO with high selectivity (up to 97%), high efficiency (Φ_{CO}s of 28% and 25%, respectively: BIH as a reductant), and high durability (TON_{CO}s of 5232 and 6038, respectively: BIH as a reductant) which are the largest TONs for CO_2 reduction using supramolecular photocatalysts in homogeneous solutions. The absence of negligible accumulation of the mono-reduced form of the photosensitizer indicates fast electron transfer to the catalyst unit(s) through the relatively large bridging ligand, and is proposed to contribute to the outstanding photocatalytic properties of the new species, including their durability. The relevant photocatalytic behaviour of the new systems indicates new avenues for the design of extended bridging ligands capable of efficiently and functionally integrate photosensitizers and catalysts towards the preparation of new, larger supramolecular photocatalysts for selective CO_2 reduction.

Introduction

Increase of atmospheric CO_2 concentration arising from the mass consumption of "fossil resources" as energy source causes serious problems, i.e., global warming and shortage of carbon and energy resources.[1, 2] This situation, in connection with the increasing global energy consumption, makes essential for our society to find new, sustainable ways to obtain a huge amount of energy without increase of CO_2 emission. Solar light is a promising candidate as a renewable energy source.[3,4] Conversion of CO_2 into energy-rich chemicals, such as CO and HCOOH, by using solar light as energy source possibly can provide a solution to both shortages of carbon and energy resources and global warming.[5]

To this goal, photocatalytic reduction of CO_2 using metal complexes which can act as a redox photosensitizer (PS) and a catalysts (CAT), has been extensively investigated.[6,7] The PS promotes photochemical electron transfer from an electron donor to the CAT. Suitable PS, which induces an efficient photocatalytic reaction via the reductive quenching process of the its excited state, should exhibit strong absorption in visible region for efficiently utilizing solar light, and its excited state should have a relatively long lifetime, strong oxidation power in the excited state, and high stability of the one-electron reduced species.[8] Ru(II) polypyridine complexes fulfil all the above mentioned requirements and are widely employed in the photocatalytic CO_2 reduction. The CAT for CO_2 reduction accepts and accumulates multiple electrons from PS and should show high selectivity of CO_2 reduction against competitive H_2 evolution. Various Re(I) diimine carbonyl complexes have been reported as such CATs.[9]

In this research area, multinuclear metal complexes, so-called "supramolecular photocatalysts", have been widely studied in the recent years.[10] The supramolecular photocatalysts contain both units, i.e. PS and CAT units, in one supramolecular photocatalyst, connected one another by a bridging ligand (BL). [11] A rapid electron transfer from the

photochemically reduced PS unit - which can be produced upon electron transfer from a sacrificial reductant or from an electrode in a photoelectrochemical cell[12] - to the CAT unit can proceed across BL:[13] this can lead to higher performances of the supramolecular photocatalysts and their higher durability compared to a mixed system of the corresponding mononuclear metal complexes. The photocatalysis behaviour of the supramolecular photocatalysts strongly depends on the properties of BL: for example, most of the efficient supramolecular photocatalysts reported in literature for CO_2 reduction are made of Ru(II) PS and Re(I) CAT containing a non-conjugated bridging ligand in which the metal chelating fragments (usually, polypyridine ligands) are connected by an alkyl chain,[14] typically an ethylene group. In fact, introduction of a conjugated chain as a substituent of the diimine ligand of the Re(I) CAT unit induces shift of its reduction potential to more positive values, which causes lower catalysis activity of the Re unit. This limitation in BL design inhibits diversification of structures of supramolecular photocatalysts and poses severe restrictions for the development of the supramolecular photocatalytic systems, so causing a paradigmatic problem for development of the whole research field. On the other side, because of the shortness of ethylene chains, back electron transfer between PS and CAT can occur, so limiting the efficiency of the overall process: extended, large bridging ligands would therefore be desirable.

We now propose a new BL (**bpy₃Ph**) suitable for constructing various supramolecular photocatalysts. This BL is a phenylene ring with three ethylene chains in 1, 3, and 5 positions, of which the other terminals are connected with 2,2'-bipyridine moieties (Chart 1). In BL all of the 2,2'-bipyridine moieties are equivalent, and various trinuclear metal complexes with different ratios of different metal centers can be selectively synthesized by using relatively simple step-by-step synthetic methods as described below. The distances among the metal-complex units connected by this new BL are much longer compared to those of the reported
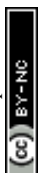
supramolecular photocatalysts in which each metal-complex unit are connected by ethylene chain(s).[15,16,17] This and the rigidity of the phenyl ring should reduce back electron transfer via direct collision of the photosensitizer unit with the reduced catalyst unit. A non-conjugated chain such as the ethylene chain between PS and CAT units is necessary to keep reduction power of the CAT.[15] However, since the three ethylene chains bearing the metal center units are covalently linked to one another through one aromatic ring of which carbons in the 1, 3, and 5 positions have strong electronic interaction, trough-bond forward electron transfer could be promoted by the large electronic interactions between the metal-based units.[13b] We can anticipate that this is indeed what occurs. Syntheses, photophysical and electrochemical properties, and photocatalytic abilities of trinuclear Ru(II)-Re(I) complexes based on this new BL, in which the ratio of the Re(I) and Ru(II) centers is 1:2 or 2:1 (Chart 1), are reported.
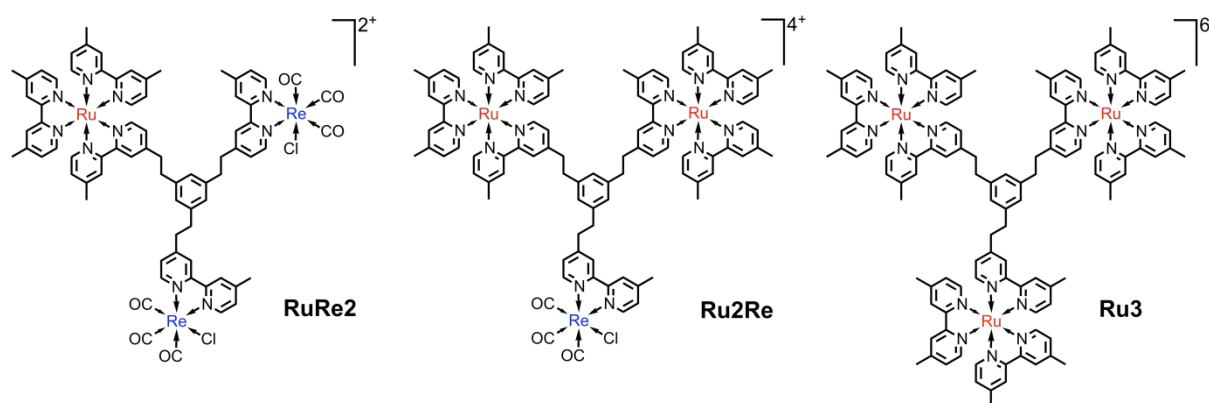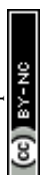

Chart 1 Structures and abbreviations of the synthesized trinuclear complexes used as PS-CAT supramolecular photocatalysts (**RuRe2 and Ru2Re**), together with **Ru3**, used as a model. The counter anions are PF$_6^-$.

Results and Discussion

Synthesis

The synthesis of the novel bridging ligand **bpy₃Ph** was accomplished in one step using 4,4'-dimethyl-2,2'-bipyridine (dmb) and 1,3,5-tris(bromomethyl)benzene. One of the methyl positions of dmb was lithiated using commercially available lithiumdiisopropylamide (LDA) slowly added to the dmb solution at -33°C. After that, a THF solution of 1,3,5-tris(bromomethyl)benzene was added dropwise and the resulting mixture was left stirring overnight at room temperature.[18] Chromatography column on silica of the crude resulted in the isolation of the product **bpy₃Ph**. The isolated yield was 57%. The characterization was performed by NMR spectroscopy (Figure S1). The signal of the aliphatic protons of 1,3,5-tris(bromomethyl)benzene (δ = 4.45 ppm) was absent in the product spectrum, but it is present a singlet signal at δ = 2.82 ppm for all the twelve protons of the ethylene chain.

The ligand **bpy₃Ph** has been employed for the preparation of three different multinuclear complexes by using step-by-step coordination of Ru(II) and/or Re(I) precursor complexes (Scheme 1). By using different molar ratio between the ligand and the cis-[Ru(dmb)$_2$Cl$_2$·2H$_2$O] metal complex, the **Ru**, **Ru2** and **Ru3** species have been prepared. In all the cases the reaction procedure gave a mixture of complexes, subsequently separated by ionic-exchange chromatography. The successive reactions of the complexes, **Ru** and **Ru2**, containing respectively two and one free dmb-type moieties, with Re(CO)$_5$Cl gave the desired **RuRe2** and **Ru2Re** complexes (Scheme 1). All of yields of the trinuclear complexes were reasonably high as shown in Scheme 1.
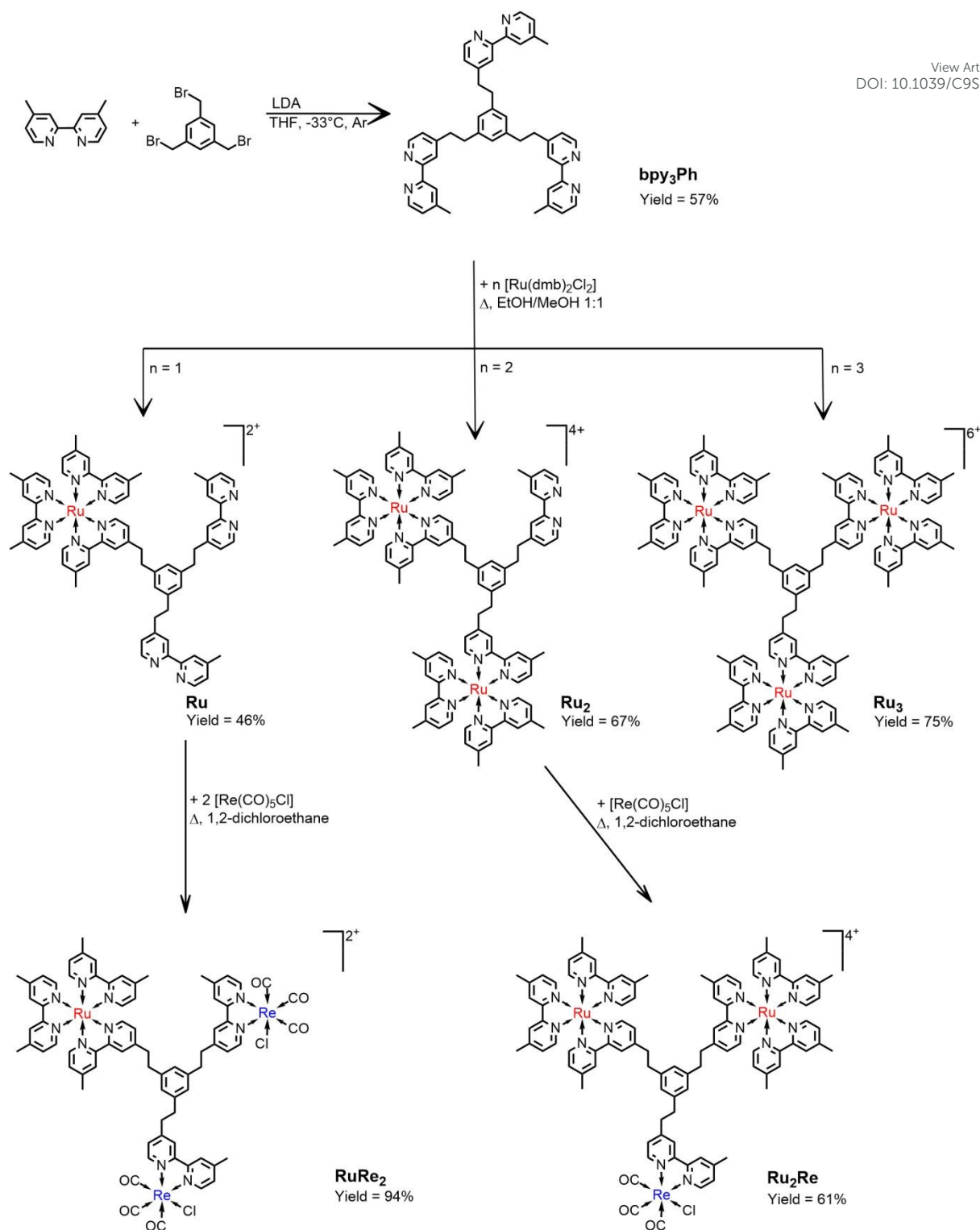
Scheme 1. Schematization of the synthetic routes

Absorption Spectra and Photophysical Properties

UV-vis absorption spectra of the complexes are shown in Figure 1. The band at λ_{max} = 460 nm was observed in all the complexes, and is attributed to the spin-allowed metal-to-ligand charge transfer (MLCT) band of the Ru(II) centre(s). The shapes of the absorption spectra of all the new compounds are very similar one another and the absorption coefficient is dependent on the number of the Ru(II) unit(s) (see Table 1). The stronger absorption band at λ_{max} = ~ 285 nm can be assigned mainly to the π-π* transition of the diimine moieties. The [1]MLCT band of the Re(I) subunit(s) should contribute to the absorption in the range λ_{max} = 350-390 nm.[19,20] Noteworthy, the absorption spectrum of each multinuclear species closely overlaps the calculated weighted sum of the absorption spectra of the relevant individual monomer components (see Figure 1), so indicating that there is no strong electronic interaction among metal centres in the multicomponent compounds.
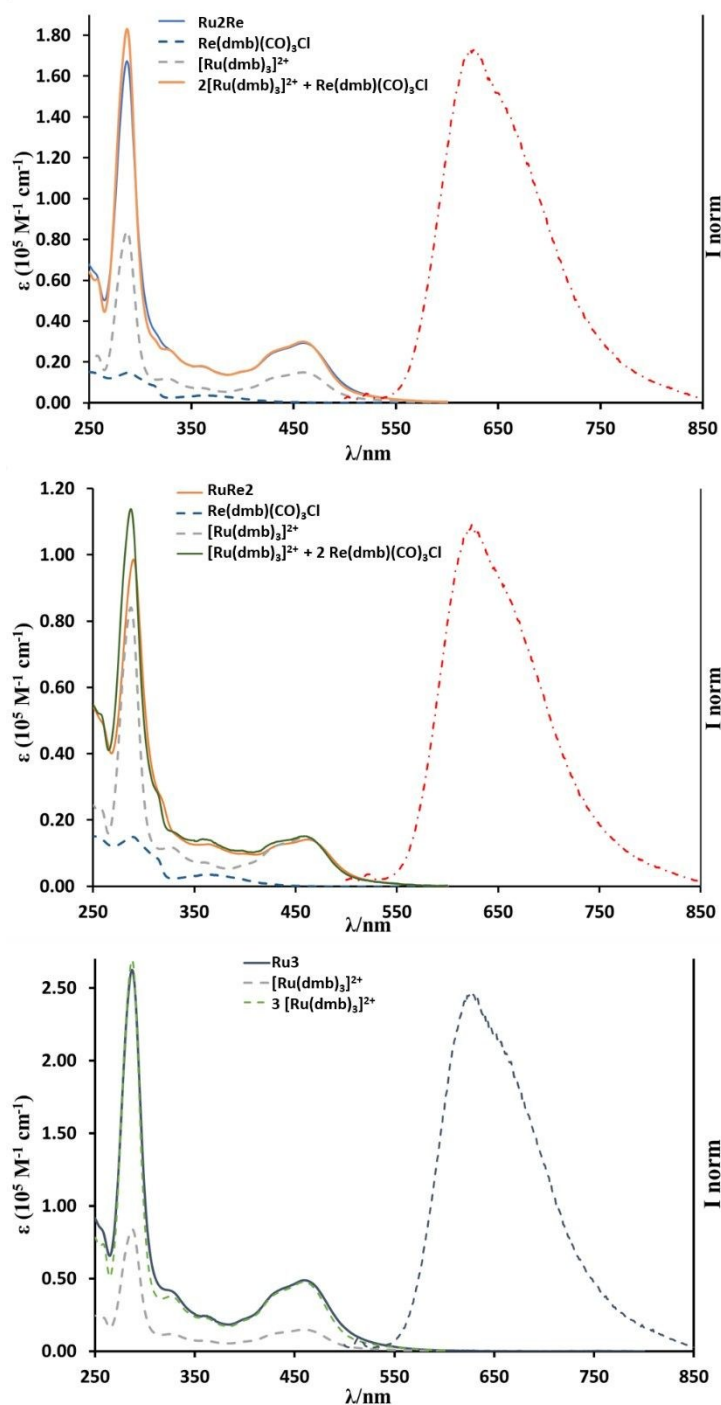
Chemical Science Accepted Manuscript

Fig. 1 UV-Vis absorption spectra of **RuRe2** (top), **Ru2Re** (middle) and **Ru3** (bottom) in MeCN at room temperature. The absorption spectra of the model species Ru(dmb)$_3^{2+}$ and Re(dmb)(CO)$_3$Cl are also shown for comparison purposes, along with the calculated weighted sum spectra of the isolated components (see text for details). Emission spectra of **RuRe2** (top), **Ru2Re** (middle), and **Ru3** (bottom) in MeCN are also shown on the right side of each panel. Excitation wavelength is 450 nm.

Figure 1 also shows emission spectra of **RuRe2**, **Ru2Re**, and **Ru3** excited at λ_{ex} = 450 nm: all the trinuclear complexes exhibit an emission band around 625 nm, similar to that of $[Ru(dmb)_3]^{2+}$, which is attributed to the ^{3}MLCT excited state of the Ru(II) unit(s). Table 1 summarizes photophysical data of all the complexes. The emission spectra, lifetimes and quantum yields of **RuRe2** and **Ru2Re**, independently of the presence of Re(I) unit(s) in their structure, are very similar to those of **Ru3**, **Ru2**, and **Ru**. The shapes of the emission spectra of the multinuclear compounds are independent of excitation wavelength, at least in the range 350-530 nm. These results clearly indicate that there is no strong electronic interaction between the excited Ru unit and the others, and intramolecular electron transfer from the excited Ru unit to the Re unit as well as self-quenching of the excited Ru units do not occur in the trinuclear species. Excitation spectra of **Ru2Re** and **RuRe2** overlap with their respective absorption spectra, so suggesting that energy transfer from the ^{3}MLCT state of the Re(I) unit(s) (responsible for the 600 nm emission of the model species $Re(dmb)(CO)_3Cl$ reported in Table 1) to the ^{3}MLCT state of the low-lying Ru(II) unit(s) largely takes place in **RuRe2** and **Ru2Re** when the Re unit is excited. However, due to the small absorption of the Re(I) unit in comparison to the absorption of the Ru(II) units (see data in Table 1) and the less intense intrinsic emission of the Re units, we cannot state if such energy transfer is effectively quantitative.

Table 1 Photophysical properties measured in deaerated MeCN[(a)]

	Absorption	Luminescence		
	λ_{max} / nm (ε_{460} / M^{-1}cm^{-1})[(b)]	λ_{max} / nm	τ / ns [(c)]	Φ_{em} [(c)]
Ru	460 (14760)	624	878 (120)	0.085 (0.016)
Ru$_2$	460 (31180)	625	851 (115)	0.086 (0.016)
Ru$_3$	460 (44500)	625	847 (117)	0.087 (0.016)
RuRe$_2$	460 (14500)	624	867 (119)	0.085 (0.016)
Ru$_2$Re	460 (28550)	625	852 (117)	0.086 (0.016)
[Ru(dmb)$_3$]$^{2+}$[(d)]	458 (16300)	622	875	0.089[(e)]
Re(dmb)CO$_3$Cl	364 (3630) [(f)]	600[(g)]	49[(g)]	0.0057[(h)]

(a)   All data are measured in MeCN at 293 K. (b) Only the low energy maximum is reported. (c) Data in parenthesis refer to air-equilibrated solution. (d) From reference 21 (e) From reference 22. (f) From reference 23. (g) From reference 24. (h) In MeTHF.

Redox Properties

The redox behaviour of all the metal complexes synthesized are summarized in Table 2, together with data of model species. In the cyclic voltammograms (CV) and in the differential pulsed voltammograms (DPV) of the complexes (Figures S2-S5), there are different ligand-based reduction and metal-based oxidation processes. Comparing the redox data of the new complexes with those of [Ru(dmb)$_3$]$^{2+}$ and [Re(dmb)(CO)$_3$Cl] reported in literature,[23, 24, 25] it is possible to safely assign the various processes to specific subunits. On oxidation, the first reversible and the second irreversible waves of **RuRe2** and **Ru2Re** are attributable to the Ru(II) and Re(I) units, respectively. In all the other complexes, only a single oxidation process takes place until +1.60 V vs SCE, with $E_{1/2}$ within 1.14 – 1.17 V, that can be attributed to oxidation of the Ru(II) centre(s). Interestingly, the number of exchanged electrons, measured by comparison of the area of DPVs, corresponds to the number of Ru(II) centres in the structures, indicating that negligible interaction takes place between the metal centres in the

multinuclear compounds from an electrochemical viewpoint, a common behaviour for multiruthenium species built around a multichelating ligand with reduced conjugation.[26]

Table 2 Redox properties

	$E_{1/2}$, V vs SCE[(a)]				
	E_{Ox2}	E_{Ox1}	E_{Red1}	E_{Red2}	E_{Red3}
Ru		+1.15 [1]	-1.44 [1]	-1.63[1]	-1.85[1]
Ru2		+1.15 [2]	-1.43 [2]	-1.61[2]	-1.89[2]
Ru3		+1.17 [3]	-1.45 [3]	-1.60[3]	-1.92[3]
RuRe2	+1.36 irr	+1.14 [1]	-1.41[3]	-1.67[1]	-1.88[1]
Ru2Re	+1.38 irr	+1.14 [2]	-1.42[3]	-1.58[2]	-1.85[2]
[Ru(dmb)₃]²⁺[(b)]		+1.10 [1]	-1.45[1]		
[Re(dmb)(CO)₃Cl][(c)]		+1.36 irr	-1.43 [1]		

(a) Electrochemical Properties measured at room temperature in MeCN containing 0.1 M TBAH. All values are obtained using the redox couple ferrocene/ferrocenium (395 mV vs. SCE in acetonitrile) as internal reference. The numbers in parentheses refer to the number of exchanges electrons. Irr indicates an irreversible process: in this case, the E values reported in table refer to peak potentials in pulse voltammetry experiments. (b) From reference 27. (c) From reference 24.

On reduction, a series of reversible processes takes place for all the complexes, at potentials that are typical of successive reductions of the various dmb ligands coordinated to a single metal centre. For example, in **Ru**, the three successive reduction processes are assigned to successive one-electron reduction of the three polypyridine ligands coordinated to the Ru(II) centre, including the one belonging to the bridging ligand. For **Ru2** and **Ru3**, all the reduction processes involve two and three electrons, respectively: in both cases, the first process is assigned to simultaneous one-electron reduction of polypyridine ligands coordinated to different metal centres (two and three metal centres in **Ru2** and **Ru3**, respectively); the second and third reduction processes are assigned to simultaneous one-electron reduction of the not yet reduced coordinated dmb-type ligands. In the mixed-metal

Ru2Re and **RuRe2** complexes, the assignment of the first reduction process – involving three simultaneous one-electron processes - follows that for **Ru3**, whereas the number of exchanged electrons for the second and third reduction processes is reduced compared to the number of electrons involved in the first reduction process, because the Re(I) centre(s) have a single dmb-type ligands. It is noteworthy that the reduction potential of the Re unit and the first reduction potential of the Ru unit(s) are very similar each other in the **Ru2Re** and **RuRe2**. The reduction patterns of the new compounds, like their oxidation behaviour, confirm that each metal-based subunit is electrochemically independent of the presence of the others in the multicomponent arrays.

Photocatalysis for CO$_2$ reduction

Photocatalytic reactions for the reduction of CO$_2$ were performed using both **Ru2Re** and **RuRe2** as supramolecular photocatalysts. In order to achieve the same light-absorbing abilities between two systems, so normalizing the light absorption and allowing a direct comparison of the properties, the concentrations of the PS units were adjusted as 50 μM in the photocatalytic reactions, i.e. [**Ru2Re**] = 25 μM and [**RuRe2**] = 50 μM were selected. In a typical run, a 3 mL CO$_2$-saturated mixed solution of *N*,*N*-dimethylacetamide-triethanolamine (DMA-TEOA; 5:1 v/v) containing **RuRe2** (50 μM) and 1,3-dimethyl-2-phenyl-2,3-dihydro-1*H*-benzo[d]imidazole (BIH; 0.1 M) as a sacrificial electron donor was irradiated using a LED light source (530 nm, 4 mW), giving CO almost selectively (Figure 2b). After 20-h irradiation, turnover number for CO production (TON$_{CO}$) reached 1850 based on the **RuRe2** used. The selectivity of the CO formation was Γ_{CO} = 92%. Since CO is a two-electron reduced compound of CO$_2$ and BIH has been reported to function as a two-electron donor, [28]CO formation of TON$_{CO}$ = 1850 means the consumption of 92.5 mM (= 0.05 × 1850) of BIH, which is 92.5% of
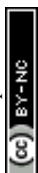
BIH added originally (100 mM). This should be one of the reasons of slower CO formation at longer irradiation. Therefore, to observe the potential durability of **RuRe2**, the photocatalytic reaction was conducted using a 1/5 concentration of **RuRe2** (10 μM) with longer irradiation time (Figure S6). After 60-h irradiation, TON_{CO} reached 5232. After the irradiation for 60 h, further irradiation did not make additional CO in both cases using **Ru2Re** and **RuRe2** even though an enough amount of BIH still remained in the reaction solution. This is one of the largest turnover numbers of CO_2 reduction using photocatalysts in homogeneous solutions. It is noteworthy that the mixed systems of separated PSs and CATs, which reported tens of thousands TON only based on catalyst, contain hundreds-to-thousands-times concentration of PS compared with CAT (in the present case, obviously the PS-CAT ratio is 1:2 for **RuRe2** and 2:1 in **Ru2Re**). In such mixed systems, TONs based on the PS concentration used are only tens or less than that, which are much smaller TON compared to the present case for the supramolecular photocatalyst **RuRe2**. The quantum yield for CO production was determined as Φ_{CO} = 25% using 480-nm light (light intensity: 1.0×10^{-8} einstein s^{-1}). Figure 3 shows absorption spectral changes during irradiation; it can be noted that only negligible changes occur.

In the system using $[Ru(dmb)_3]^{2+}$-type PSs and BIH as a sacrificial electron donor, it has been reported that the initial step of photocatalytic reaction is photo-induced electron transfer from BIH to the excited PS giving its one-electron reduced species (OERS) which exhibits characteristic shape of spectrum at λ_{max} ~ 500-540 nm.[10] Since, in Figure 3, accumulation of the OERS species was not significantly observed during the photocatalytic reaction, intramolecular electron transfer from OERS of the PS unit to the CAT units should be fast and not the rate-limiting step.
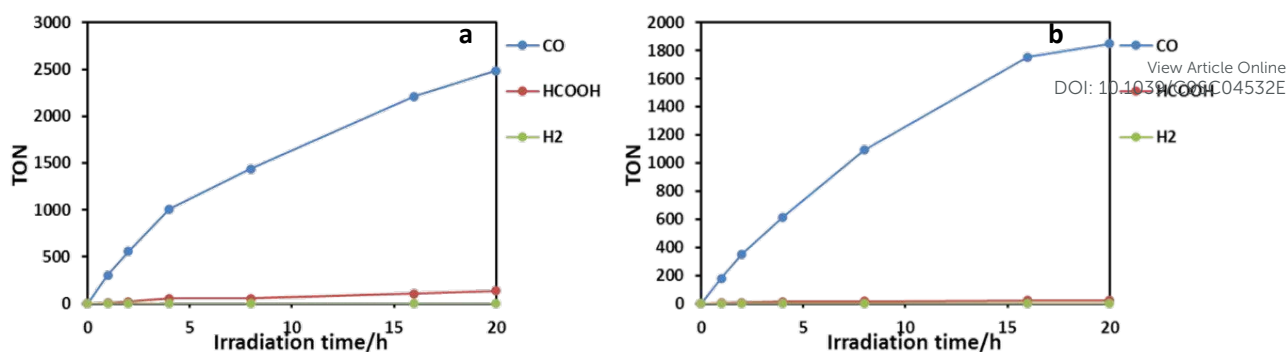
Fig. 2 Photocatalytic formation of CO (blue line), formic acid (red line) and H_2 (green line) as function of irradiation time using (a) **Ru2Re** and (b) **RuRe2**: CO_2-saturated DMA-TEOA (5:1 v/v, 3 mL) solutions containing **Ru2Re** (25 μM) or **RuRe2** (50 μM) and BIH (0.1 M) were irradiated at λ_{ex} = 490-615 nm.
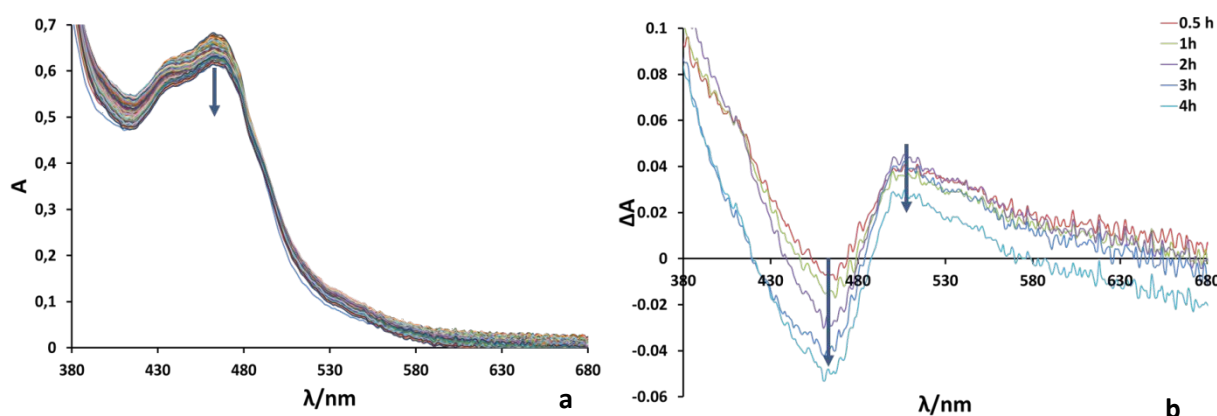

Fig. 3 (a) UV-vis absorption spectra during irradiation of a DMA-TEOA (5:1 v/v) solution containing **RuRe2** (50 μM) and BIH (0.1 M) at λ_{ex} = 480 nm for 240 min at 1-min intervals. (b) UV-vis differential absorption spectra between before and after irradiation.

     Ru2Re also displayed superior photocatalytic activities: TON_{CO} = 2486 and Γ_{CO} = 90%, and Φ_{CO} = 28% in the case of [**Ru2Re**] = 25 μM (Figure 2a), and TON_{CO} = 6038 and Γ_{CO} = 81% in the case of [**Ru2Re**] = 5 μM. During photocatalysis, no significant UV-vis absorption spectral change was also observed. For comparison, we also checked photocatalysis of the reported binuclear complex (**RuRe**) of which one Ru(II) photosensitizer and one Re(I) catalyst units are

15

connected with an ethylene chain without the phenyl group in the same reaction condition: TON_{CO} = 3657 in the case of [**RuRe**] = 10 µM (Figure S8). It is noteworthy that TON_{CO} of **Ru2Re** based on the Re unit was over 6000, which is much higher compared to those in the case of **RuRe** even though both supramolecular photocatalysts have the same number of the Re unit. The researches related to this difference of durability among the supramolecular photocatalysts are in progress in our laboratory.

Table 3. Photocatalytic properties of **Ru2Re** and **RuRe2**.[a]

|		Product / µmol (TON)[b]			Φ_{CO} / %[c]	Γ_{CO}	k_q[e]	η_q
		CO	HCOOH	H_2		%[b,d]	10^7 M^{-1}s^{-1}	%[f]
	Ru2Re	186.5 (2486 ± 12)	20.2 (269)	0.01	28 ± 0.6	90	83 ± 0.8	99
	Ru2Re[g]	90.6 (6038 ± 18)	21.7 (1447)	0.02	-	81	83 ± 0.8	99
BIH	**RuRe2**	277.4 (1850 ± 10)	3.3 (22)	~0	25 ± 0.5	99	80 ± 2.6	99
	RuRe2[h]	157.0 (5232 ± 14)	5.3 (177)	~0	-	97	80 ± 2.6	99
	RuRe[i]	110.0 (3657 ± 29)	1.1 (36)	0.03	30 ± 1.1	99	120 ± 0.5	99
BNAH	**Ru2Re**	17.5 (216 ± 5)	13.0 (77)	0.8	6.9 ± 0.9	56	2.0 ± 0.3	63
	RuRe2	33.7 (225 ± 6)	8.6 (57)	0.2	8.3 ± 1.2	79	2.2 ± 0.5	67

[a]CO_2-saturated DMA-TEOA (5:1 v/v) solution containing **Ru2Re** (25 µM) or **RuRe2** (50 µM) and a sacrificial electron donor (0.1 M) was irradiated. [b]3-mL solution was irradiated for 20 h using a LED (530 nm, 4 mW) as a light source. TONs are calculated based on the photocatalyst used. [c]4-mL solution was irradiated at λ_{ex} = 480 nm (light intensity: 1 × 10^{-8} einstein s^{-1}). [d]The selectivity for CO production. [e]Quenching rate constants for emissions from the photosensitizer unit by a sacrificial electron donor obtained from linear Stern-Volmer plots and their lifetimes. [f]Quenching fractions for emissions from the photosensitizer unit by a sacrificial electron donor (0.1 M) calculated as $0.1k_q\tau_{em} / (1 + 0.1k_q\tau_{em})$. [g][**Ru2Re**] = 5 µM, 60-h irradiation. [h][**RuRe2**] = 10 µM, 60-h irradiation. [i][**RuRe**] = 10 µM, 60-h irradiation.

Table 3 summarizes the photocatalytic abilities of **Ru2Re** and **RuRe2** by using BIH, which is a two-electron donor, or 1-benzyl-1,4-dihydronicotinamide (BNAH), which is a one-electron donor.[28] In the cases using BNAH as a sacrificial electron donor instead of BIH, photocatalytic
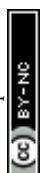
CO_2 reduction also proceeded with relatively high durability and efficiency even though these values are less than those using BIH. The reason of the difference in photocatalytic activities between using BNAH and BIH has already been reported as follows: i) because of stronger reduction power of BIH ($E_{1/2}^{ox}$(BIH/BIH·$^+$) = 0.33 V vs. SCE)[29] than BNAH ($E^{\circ ox}$(BNAH/BNAH·$^+$) = 0.57 V),[30] quenching efficiencies of the excited Ru unit by BNAH (η_q = 67% and 63% in the case using **RuRe2** and **Ru2Re**, respectively) were lower than that by BIH (η_q = 99% in both cases); ii) BIH is a two-electron donor while BNAH is a one-electron donor (eqs. 1 and 2); iii) The one-electron-oxidized, deprotonated, and dimerizing compounds of BNAH, i.e., 4,4'- and 4,6'-BNA$_2$s, efficiently and reductively quench the excited Ru unit. However, they do not work as reductants owing to high stability of their one-electron-oxidized product (BNA$_2^+$•) and rapid back-electron transfer from the reduced Ru unit to BNA$_2^+$• (eq. 3). Therefore, accumulation of the BNA$_2$ should lower the yield of reduction of the excited Ru unit by BNAH, as competitive quenchers for excited Ru quenching. In the cases using BIH, on the other hand, the oxidized compound of BIH (BI$^+$) does not affect the photocatalytic reactions. Note also that it is known that proton release is much faster for the oxidized BIH than for the oxidized BNAH,[28] and this can also contribute to the best performance of BIH as a sacrificial donor.


(1)

(2)

(3)
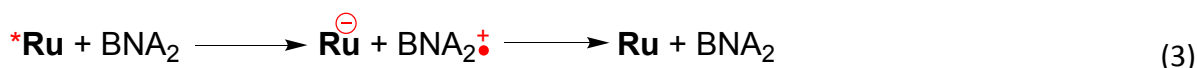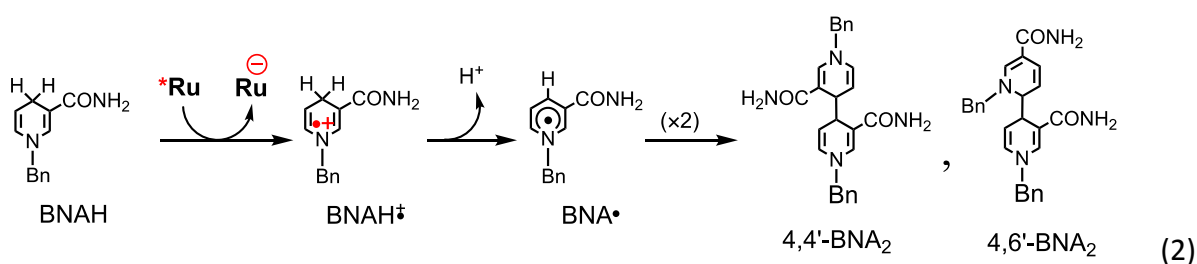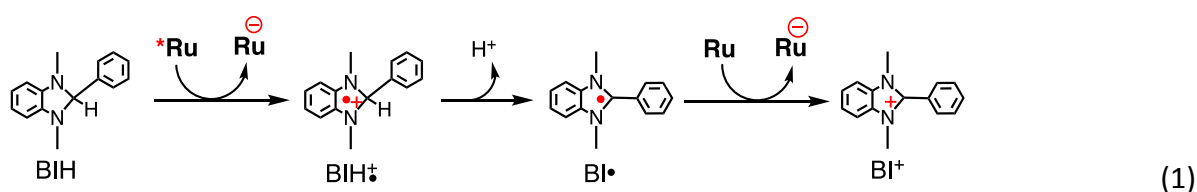
Conclusions

A series of trinuclear metal complexes have been synthesized, based on a new tris-chelating bridging ligand, in which three bipyridine-decorated ethylene chains are connected one another by a central phenyl ring. The trinuclear metal complexes so prepared contain $Ru(dmb)_3$-type chromophores and $Re(dmb)(CO)_3Cl$-type catalysts for CO_2 reduction in different ratios, by made-to-order synthesis, therefore giving rise to supramolecular photocatalysts for CO_2 photoreduction. The results indicate that:

- the various metal subunits of the supramolecular catalysts keep their own light absorption and redox properties in the supermolecule assemblies and electronic interactions between the various metal centres are negligible;

- fast electron transfer between reduced chromophores and the catalyst unit(s) occurs, in spite of the relatively large metal-metal separation due to the bridging ligand structure;

- quite efficient visible light-induced catalytic CO formation occurs in mixed-metal Ru(II)-Re(I) supramolecular photocatalysts, with outstanding turnover numbers (over 6000 in one case), high selectivity and durability: such high TONs are among the highest values for photocatalytic CO_2 reduction in homogeneous solutions. This TON_{CO} is almost twice as large as the previous most durable photocatalyst, the binuclear complex consisting of Ru(II) photosensitizer and the Re(I) catalyst units, which are similar units but are connected with an ethylene chain without the phenyl group.

All together, these achievements represent a breakthrough in the design of novel supramolecular photocatalysts, allowing to overcome the size limit in bridging ligand represented by the ethylene bridges most commonly used in efficient PS-CAT supramolecular photocatalysts reported up to now. Actually, the present results indicate that new bridging ligands in which aromatic moieties are judiciously incorporated within the bridging ligand

Chemical Science Accepted Manuscript
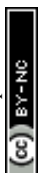
structure can allow to obtain fast long-range electron transfer, suitable for the photocatalytic

process, without affecting the behaviour of the catalytic subunit(s). This can open new

avenues for the design of new, more efficient and stable supramolecular photocatalysts for

selective CO_2 photoreduction.

Acknowledgements

Chemical Science Accepted Manuscript

References

1 T. R. Karl and K. E. Treberth, *Science*, 2003, **302**, 1719-1723.

2 H. Akimoto, *Science*, 2003, **302**, 1716-1719.

3 N.S. Lewis and D.G. Nocera, *Proc. Natl. Acad. Sci. USA,* 2006, **103**, 15729-15735.

4 S. Berardi, S. Drouet, L. Francàs, C. Gimbrt-Suriñach, M. Guttentag, C. Richmond, T. Stoll and A. Llobet, *Chem. Soc. Rev.*, 2014, **43**, 7501-7519.

5 S. C. Roy, O. K. Varghese, M. Paulose and C. A. Grimes, *ACS Nano*, 2010, **4**, 1259-1278.

6 Y. Yamazaki, H. Takeda and O. Ishitani, *J. Photochem. Photobiol. C*, 2015, **25**, 106-137.

7 S. Das and W. M. A. Wan Daud, *RSC adv.*, 2014, **40**, 20856-20893.

8 A. Ito and T.J. Meyer, *Phys. Chem. Chem. Phys.*, 2012, **14**, 13731-13745.

9 (a) J. Hawecker, J.-M. Lehn and R. J. Ziessel, *Chem. Soc., Chem. Commun.* 1983, 536-538;

   (b) J. Hawecker, J.-M. Lehn and R. Ziessel, *Helv. Chim. Acta*, 1986, **69**, 1990-2012;

   (c) K. Koike, H. Hori, M. Ishizuka, J. R. Westwell, K. Takeuchi, T. Ibusuki, K. Enjouji, H. Konno, K. Sakamoto and O. Ishitani, *Organometallics*, 1997, **16**, 5724-5729;

   (d) H. Hori, F. P. A. Johnson, K. Koike, O. Ishitani and T. Ibusuki, *J. Photochem. Photobiol. A: Chem.*, 1996, **96**, 171-174.

10 Y. Tamaki and O. Ishitani, *ACS Catal.*, 2017, **7**, 3394-3409 and refs. therein.

11 V. Balzani and F. Scandola, *Supramolecular Photochemistry*, Horwood, Chichester (UK), 1991.

12 A. Juris, V. Balzani, F. Barigalletti, S. Campagna, P. Belser and A. von Zelewski, *Coord. Chem. Rev.*, 1988, **84**, 85-277.

13 (a) K. Koike, D. C. Grills, Y. Tamaki, E. Fujita, K. Okubo, Y. Yamazaki, M. Saigo, T. Mukuta, K. Onda and O. Ishitani, *Chem. Sci.*, 2018, **9**, 2961-2974;

   b) Y. Yamazaki, K. Ohkubo, D. Saito, T. Yatsu, Y. Tamaki, S. i. Tanaka, K. Koike, K. Onda and O. Ishitani, *Inorg. Chem.*, in press, DOI: 10.1021/acs.inorgchem.9b01256.

14 K. Ohkubo, Y. Yamazaki, T. Nakashima, Y. Tamaki., K. Koike and O. Ishitani, *J. Cat*, 2016, **343**, 278-289.

15 B. Gholamkhass, H. Mametsuka, K. Koike, T. Tanabe, M. Furue and O. Ishitani, *Inorg. Chem.*, 2005, **44**, 2326-2336.

16 Y. Kuramochi and O. Ishitani, *Inorg. Chem.,* 2016, **55**, 5702-5709.

17 S. Meister, R. O. Reithmeier, A. Ogrodnik and B. Rieger, *ChemCatChem*, 2015, **7**, 3562-3569.

18 R. Dorta, R. Dorta, L. J. W. Shimon and D. Mistein, *Inorg. Chem.,* 2004, **43**, 7180-7186.

19 (a) "Photochemistry and Photophysics of Coordination Compounds: Rhenium": A. Kirgan, B. P. Sullivan and D. P. Rillema in *Photochemistry and Photophysics of Coordination Compounds II*, (Eds.: V. Balzani, S. Campagna), Springer, Berlin, 2007, **281**, 45-100; (b) A. J. Lees, *Chem*. *Rev.*, 1987, **87**, 711-743.

20 (a) J. Rohacovaa and O. Ishitani, *Dalton Trans.*, 2017, **46**, 8899-8919; (b) A. Juris, S. Campagna, I. Bidd, J. M. Lehn and R. Ziessel, *Inorg. Chem.*, 1988, *27* (22), 4007–4011.

21 D. S. Tyson and F. N. Castellano, *J. Phys. Chem. A*, 1999, **103** (50), 10955-10960.

22 Y. Tamaki, K. Watanabe, K. Koike, H. Inoue, T. Morimoto and O. Ishitani, *Faraday Discuss.*, 2012, **155**, 115-127.

23 L. A. Worl, R. Duesing, P. Chen, L. Della Ciana, T. J. Meyer, *J. Chem. Soc., Dalton Trans.* 1991, **0**, 849-858.

24 M. Furue, M. Naiki, Y. Kanematsu, T. Kushida and M. Kamachi, *Coord. Chem. Rev.*, 1991, **111**, 221-226.

25 K. Koike, S. Naito, S. Sato, Y. Tamaki and O. Ishitani, *J. Photochem. Photobiol. A: Chem.*, 2009, **207**, 109-114.

26 (a) E. La Mazza, F. Puntoriero, F. Nastasi, B. Laramée-Milette, G. S. Hanan and S. Campagna, *Dalton Trans.*, 2016, **45**, 19238-19241; (b) B. Laramée-Milette, F. Nastasi, F. Puntoriero, S. Campagna and G. S. Hanan, *Chem. Eur. J.*, 2017, **23**, 16497-16504; (c) F. Puntoriero, S. Serroni, F. Nastasi and S. Campagna in *Electrochemistry of Functional Supramolecular Systems*, John Wiley & Sons, Inc.: Hoboken, NJ, USA, 2010, 121–143.

27 Y. Kawanishi, N. Kitamura, Y. Kim and S. Tazuke, *Riken Q.*, 1984, **78**, 212-219.

28 Y. Pellegrin and F. Odobel, *C. R. Chimie*, 2017, **20**, 283-295.

29 E. Hasegawa, S. Takizawa, T. Seida, A. Yamaguchi, N. Yamaguchi, H. Chiba, T. Takahashi, H. Ikeda and K. Akiyama, *Tetrahedron,* 2006, **62**, 6581-6588.

30 S. Fukuzumi, S. Koumitsu, K. Hironaka and T. Tanaka, *J. Am. Chem. Soc.*, 1987, 109, 305-316.

Chemical Science Accepted Manuscript